RECOVERY OF AMMONIA, PHOSPHATE AND MAGNESIUM IONS FROM STRUVITE

Sophia Waseem Khan, Dept of Chemistry, Durham University

Laidlaw Undergraduate Research and Leadership Scholarship Programme

Abstract

This research project investigated the recovery of ammonium, phosphate and magnesium ions from struvite, $NH_4MgPO_4 \cdot 6H_2O$. An explorative study into the solubility of struvite in carbonic acid was undertaken, followed by experiments which utilised the recovered ions in the synthesis of fertilisers. The dissolution of struvite in carbonic acid was successful, as was the synthesis of ammonium bentonite. Further adjustment of the methodology for the synthesis of magnesium iron layered double hydroxides, MgFeLDH's is required to increase product yield and purity. Given the exploratory nature of this research, numerous potential directions for further study have emerged, both widespread and varied in nature. For example, research could be undertaken investigating the implementation of struvite dissolution processes in WWTPs in collaboration with chemical engineers. Moreover, it could also explore the supply chain process of getting the recovered ions to other sectors and industries.

Acknowledgements

I would like to thank Professor Chris Greenwell, Dr Catriona Sellick, Héctor Escamilla-Garcia and all the Greenwell Research Group for their guidance, support and mentorship during this project.

I would also like to extend my gratitude to the Laidlaw Foundation for this wonderful opportunity.

1. Literature Review

1.1 Struvite

Struvite, $NH_4MgPO_4 \cdot 6H_2O$, is a orthophosphate mineral which forms when an equimolar ratio of magnesium, ammonia and phosphate is present.[1] It has an orthorhombic crystal shape (see Figure 1) consisting of PO_4 regular tetrahedra, and distorted $Mg.H_2O$ octahedra, with hydrogen bonds holding the NH_4^+ cations in place, shown in Figure 2 as black dashed lines between ammonium ions.[2]

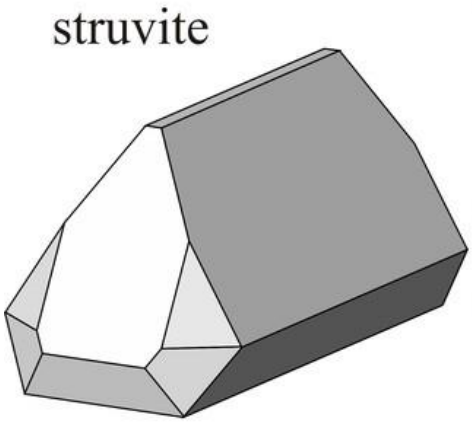

Figure 1. crystal shape of struvite [3]

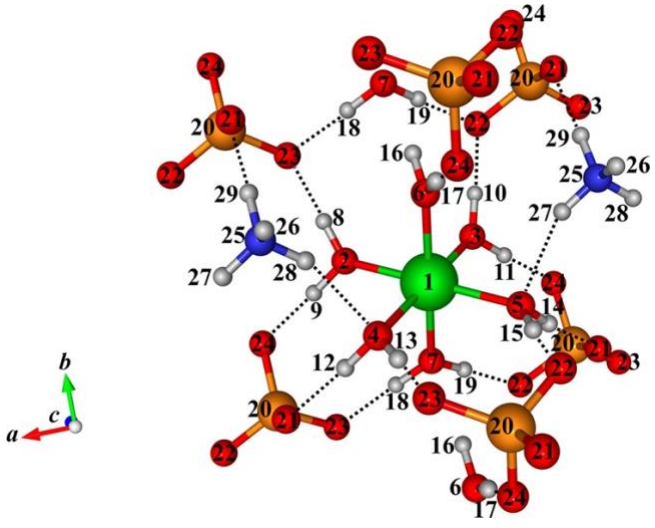

Figure 2. Fragment of struvite crystal, green, red, blue, orange, and white balls depict positions of Mg, O, N, P, and H atoms, respectively.[4]

1.2 The prevalence of struvite

Struvite forms in environments with a high percentage of decomposing organic matter. These environments include wastewater treatment plants (WWTPs) that process sewage sludge or other forms of organic waste by utilising anaerobic digestion, see appendix for more information on how a WWTP works.[5, 6] Anaerobic digestion is a favourable method of treating sewage sludge waste as the biogases, such as carbon dioxide and methane, produced can be collected and returned to the gas network.[7] The liquid product can also be repurposed because it has a high plant-nutrient content and a high pH.[8]

Significant amounts of ammonia and phosphorus are present in the solid sludge which reacts with the magnesium ions present in the wastewater, causing struvite to precipitate in the digestate discharging pipes. This causes numerous operational problems, including pipe blockages, which drastically reduces the effectiveness and efficiency of the plant as shown in Figure 3.[9]

Figure 3. Formation of Struvite in WWTP pipes

The solid sludge waste, usually containing high percentages of struvite, is primarily given to the agricultural sector to spread onto their land as a soil improver. However, this is unproven in terms of its effectiveness, its safe use, and does not fully account for the possibility of heavy metals and soluble inorganic compounds present.[10, 11]

1.3 Struvite as a source of ammonium, phosphate and magnesium 2+ ions

The Haber-Bosch process is the industrial method of ammonia synthesis, converting nitrogen and hydrogen directly to ammonia. It is a very energy and material intensive process, releasing up to 2.16 kg of carbon dioxide per kilo of ammonia,[12] 1.4% of global carbon dioxide emissions.[13] Furthermore, approximately 96% of the hydrogen required for the Haber-Bosch process is derived from fossil fuels.[14] This makes ammonia (formed via the Haber-Bosch Process) the most energy-intensive commodity chemical in the world.[15] Sourcing ammonium ions from a waste material, for example struvite, could be a much more sustainable, environmentally-friendly option.

Ammonium is also the foundation of the entire nitrogen fertiliser industry, with 80% percent of the world's supply used for this purpose.[16] The rising demand as a result of the energy crisis is increasing the price of ammonia and therefore the price of ammonia based fertilisers which in turn could lead to 323 million more people facing acute food poverty.[17] As our population is dependent on ammonia for food security and numerous other industries are reliant on ammonia (see Figure 5) it is essential that sustainable sources of ammonia are found.

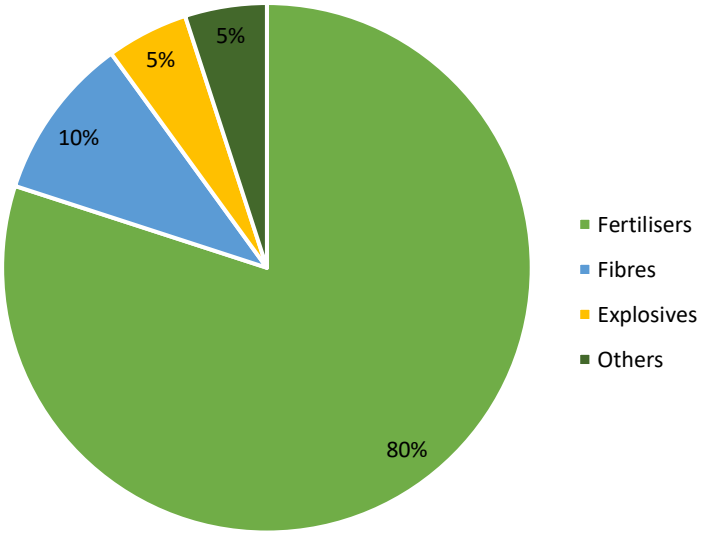

Figure 4. The Uses of Ammonia [18]

The agricultural sector is also dependent on the use of phosphates as phosphate is a critical nutrient required for plant growth.[19] Phosphorous is produced through the mining of phosphate rock, and the mining process can have a devastating environmental impact on the landscape, fresh-water quality and biodiversity.[20] Sourcing phosphate from struvite has the potential to protect these regions from environmental destruction and could be a more sustainable source of phosphate and phosphorous.

Magnesium ions have numerous applications, are biocompatible and are essential in the formation of other useful materials, such as refractory material, medical devices and automotive industry.[21] The Greenwell Group at Durham University is researching the use of magnesium ions in the formation of layered-double hydroxides (LDHs) which can be used as catalysts for the production of biofuels, as absorbents, and in ion exchange reactions.

1.4 Previous Research and Recovery Methods

The majority of existing research focuses on recovery systems which precipitate struvite as a mineral, not separately as ammonium, magnesium and phosphate ions and uses materials from other sectors besides the wastewater treatment industry. For example, Li et al. [23] have successfully recovered struvite using spent refractory brick (SRB) which is a ceramic material used in the steel industry to line kilns, furnaces and other heating systems. This study used the SRB as a source of Mg^{2+} to react with synthetic wastewater composed of ammonium chloride and disodium phosphate (pH 8.4-8.8) and tried to determine the ideal conditions for struvite precipitation. A solution of sodium carbonate, sodium sulphate, sodium sulphite and 70% nitric acid was utilised to leach the struvite. In a capped polypropylene bottle, 200 g of SRB particles was added into 1 L of DI water containing 10 mL 70% nitric acid. The bottle was then rotated at 30 ± 2 rpm for 18 ± 2 hrs in a TCLP tumbler. To obtain the struvite shown by the process in figure 5, the removal of calcium cations present in the SRB was required, forming calcium sulphite.

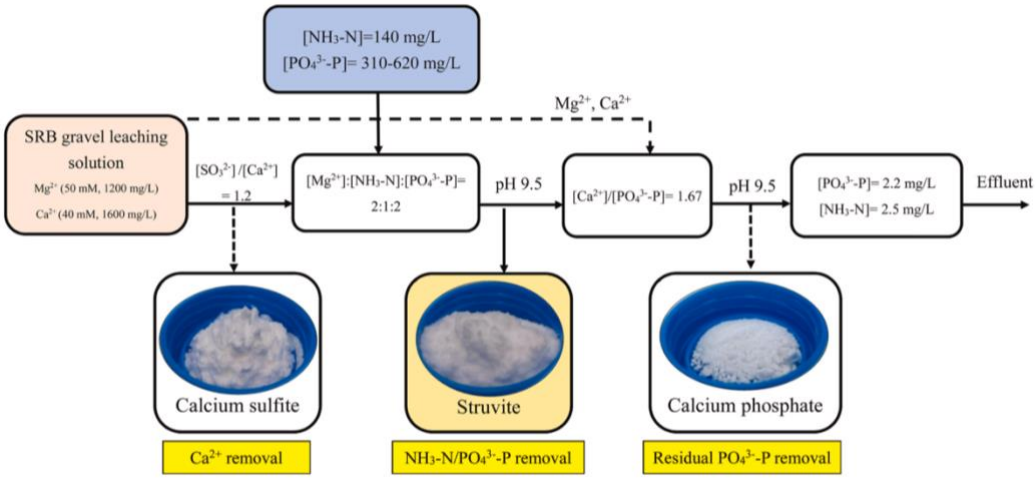

Figure 5. The chemical process utilising SRB to recover ammonium and phosphate[22]

Ammoniacal nitrogen and phosphorous as phosphate was effectively removed by the precipitation of struvite, with 2.5 mg/L equating to 98.2% of ammonia removed and 2.2 mg/L equating to 99.6% of phosphate removed. The research concluded that for the recovery of ammonia and phosphate, SRB gravels, a waste material could be effectively used in the process.

Ammonium and phosphate recovery in the form of struvite precipitation has been studied by Zin et al. [23] via the hydrolysis and incineration of sewage sludge. This study proposes an environmental and efficient pathway for struvite production with the recovery of ammoniacal nitrogen (NH^{4+}-N) and PO_4^{3-}-P from sewage sludge by two different pre-treatments.[23]

Alkaline hydrolysis, a double decomposition reaction utilising water[24] in basic conditions, of the sewage sludge breaks down the organic matter present, releasing ammonium related species into the solution. During the incineration process, the organic matter in the sewage sludge is burned, leaving behind an ash residue.[25] This ash residue, known as sewage sludge ash (SSA), contains a high concentration of phosphorus[26] which was then utilised with the NH^{4+}-N rich solution for the formation of struvite.

88.0% of the ammoniacal nitrogen was successfully recovered as struvite. Furthermore, the incineration of sewage sludge resulted in 94.1% of the PO_4^{3-}-P also successfully recovered as struvite. Chemical and spectroscopic analyses were conducted to determine the chemical nature and composition of the recovered struvite product from the sludge hydrolysate. The recovered product (see Figure 6) was found to have 12.5% of PO_4^{3-}-P, 5.3% of NH^{4+}-N, and 9.3% of Mg^{2+}. 92.6% of the recovered product contained struvite, with a very high phosphorous bioavailability and low amount of heavy metals.[23]

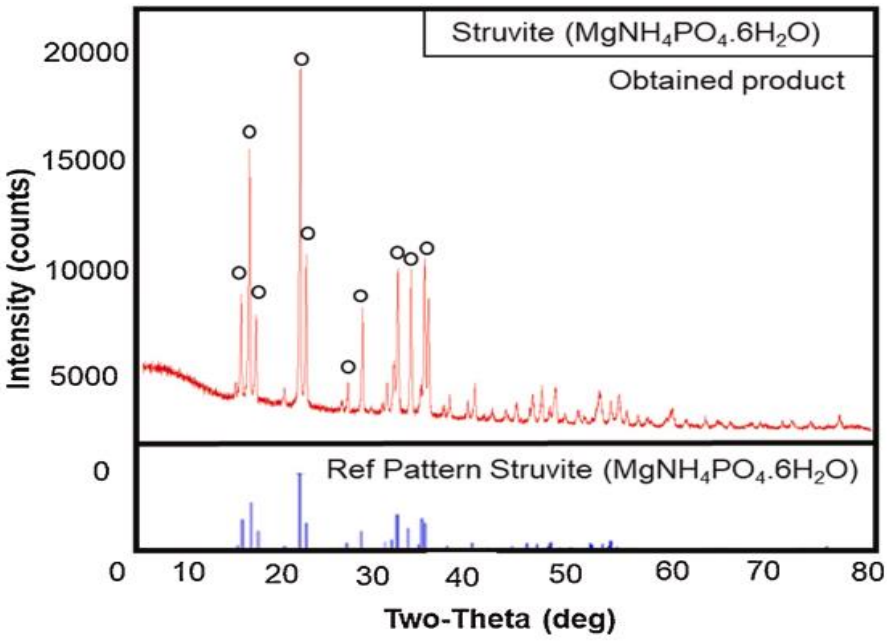

Figure 6. XRD spectra of the recovered struvite formed in comparison to a XRD struvite reference.[23]

The recovery of phosphate and phosphorous nutrients specifically through struvite precipitation has been studied at length within the present literature.[27] To maximise the amount of phosphate recovered and struvite formed with more efficiency, numerous methods, processes and technologies have been explored. For example, electrochemical struvite precipitation was accomplished with a batch monopolar reactor with optimised parameters achieving 97.3% struvite recovery, by Bhoi et al. [28]

Other research utilising electrochemical methods investigated efficient phosphate recovery from swine wastewater through the use of struvite precipitation electrolysers. The study by Wang et al.[29] also explored how pH and phosphate concentration affected the reaction rate of struvite formation, which is seen in Figure 7, with 99.51% efficiency of phosphate recovery at optimal conditions.[29]

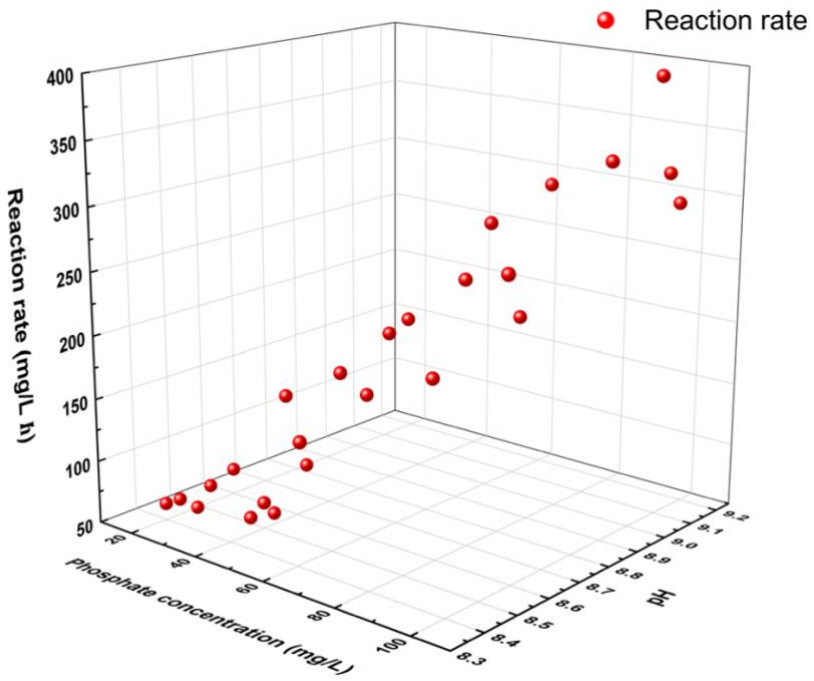

Figure 7. The reaction rate of struvite precipitation under the parameters of changing phosphate concentration and pH [29]

A differing approach researched by Jaffer et al.[30] investigated which stream in a full-scale WWTP would be most effective for lab-scale precipitation of struvite as a method of the removal of phosphorous. The centrifuge liquors were discovered to be the most suitable for this purpose. 97% phosphorous removal was achieved when the centrifuge liquor was dosed with magnesium and the pH was increased to 9.0. The liquor was dosed because the ratio of Mg:P needed to be at least 1.05:1.[31] If this ratio of Mg:P was not met, 72% phosphorous removal was observed but not exclusively as struvite.[30]

Another group of studies analysed the solubility and thermal decomposition of struvite in different solutions, such as deionised water and varying acidic solutions. The chemical equation of struvite decomposition is shown below (Equation 1).

Equation 1. The chemical decomposition of struvite [32] $MgNH_4PO_4.6H_2O \rightleftharpoons Mg^{2+} + NH_4^+ + PO_4^{3-} + 6H_2O$

One experimental method researched by Ariyanto[33] analysed the dissolution of 0.45 g of struvite in 100 ml solution at various pH's and temperatures from 25°C – 40°C with continuous stirring for 24 hrs. The solution was a mixture HCl and NaOH at differing concentrations to vary the pH per 100 ml solution. Figure 8 shows the different solubilities of struvite at varying pH's and temperatures, with the overall maximum solubility achieved at 35 °C.[33]

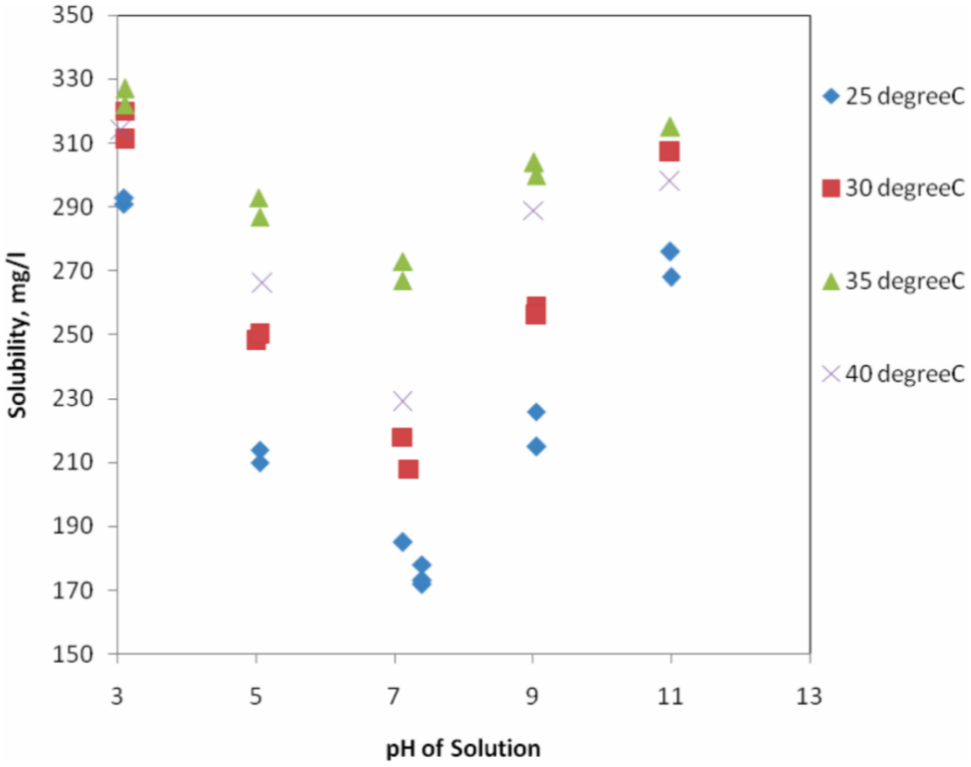

Figure 8. Solubility of Struvite for Variation Initial Solution pH at Different Temperatures.[33]

In conclusion, several factors which impact struvite solubility are pH, temperature, ion concentration and the other chemical constituents in the solution or wastewater.[34] These factors determine the supersaturation, ratio[35], see appendix for definition, while the excess supersaturation is a major aspect in predicting precipitation of a material from the liquid.[36]

2. Objectives of the Research

The primary purpose of this research is to explore the recovery of ammonium (NH_4^+) magnesium (Mg^{2+}) and phosphate (PO_3^{4-}) from struvite in a sustainable, ethical way.

By comparison with the previous methods discussed in section 1.4, this project endeavours to explore methods of ammonium, phosphate and magnesium ion recovery from struvite by using the products of anaerobic digestion, that would be readily available on a WWTP and avoids using strong, dangerous chemicals.

The experiment methodologies used were chosen based on researching and understanding the following points:

- Analysing previous studies which investigate the solubility of struvite at differing pH and temperatures.
- The exploration of the solubility of struvite in different solutions and thermodynamical conditions.
- The effect of solvent choice on the salts formed, their ease of extraction and their industrial worth and useability for redistribution and the consumer.
- Exploring the different materials which can be formed by the ions composing struvite.

3. Materials and Methodology

3.1 Experiment 1 Solubility study of struvite in carbonic acid

Experiment 1 and its counterparts were an initial explorative study into the solubility of struvite in carbonic acid. Numerous studies have explored the solubility of struvite in water but there is little data exploring the solubility of struvite in carbonic acid. Carbonic acid was chosen as the main solvent to explore as carbon dioxide is one of the main gases produced as a product of anaerobic digestion in WWTPs. If carbonic acid could dissolve struvite at a sustainable temperature and pH, it could be easily reintroduced into the wastewater treatment system, as carbon dioxide dissolved in water.

Synthetic struvite and struvite samples from Northumbria Wastewater Treatment Plant were dissolved in 100 ml of carbonic acid of pH 5 to test the ability of carbonic acid (CO_2 dissolved in water) to dissolve struvite. The samples were heated at an approximate temperature of 318.15K left for 24 hrs while stirring at 300 rpm. X-ray diffraction (XRD) graphs and images from a scanning electron microscope (SEM) were used to classify any potential products formed in the dissolution reaction and to determine what occurs to the struvite during dissolution.

EXP1.1 Dissolution of powdered synthetic struvite in carbonic acid (pH 5) open system

Powdered synthetic struvite (0.5 g) was dissolved in carbonic acid (100 ml) at pH 5with constant stirring (300rpm) at 35°C for 24hrs.

EXP 1.2 Dissolution of WWTP powdered struvite sample in carbonic acid (pH 5) in an open system

0.5 g of a powder WWTP struvite sample was dissolved in 100ml sol^n of carbonic acid at pH 5 with constant stirring of 300rpm at 35°C for 24hrs.

Both experiments 1.1 and 1.2 were undertaken in an open system (conical flask) as there was the potential of a closed system to created unsafe pressures and further reading needed to be conducted before trying a closed system experiment.

Both products were washed with deionised water, filtered by Buchner filtration, and allowed to dry at room temperature for 48hrs. This allowed the solid product to be analysed by x-ray diffraction (XRD) and scanning electron microscopy (SEM).

EXP 1.3 Dissolution of chunks of struvite in same carbonic acid soln as EXP 1.1

0.45 g of real struvite (small fragments of mineral) was dissolved in 100ml soln of carbonic acid at standard conditions.

This experiment was undertaken to observe any changes that had occurred to the WWTP struvite samples if submerged in carbonic acid soln for longer than 24hrs.

3.2 Experiment 2 Formation of ammonium bentonite

Experiment 2 endeavours to separate the ammonium cations from struvite dissolved in a 1 M HCl solution by reacting the solution with sodium bentonite, a clay mineral, potentially forming ammonium bentonite, a multi-purpose clay and fertiliser.

Ammonium bentonite was synthesised by mixing sodium montmorillonite clay with 1 M HCl struvite soln. 0.5757 g of sodium montmorillonite clay was mixed with 100 mL of the 1 M HCl struvite solution for 12 hours. This was repeated for higher masses of bentonite, 0.8571 g (1.5x the stochiometric ratio) and 1.1465 g (2x the stochiometric ratio). The product was dried at room temperature for 120 hrs.

3.3 Experiment 3 Formation of magnesium iron layered double hydroxide

Experiment 3 involved potentially making a useful product from the struvite ions, excluding ammonium. Layered double hydroxides are a multipurpose material and have numerous beneficial properties. This experiment aimed to form a magnesium iron hydroxide with the phosphate ions contained in the LDH lattice structure. SEM analysis was utilised to analysis shape of products.

The MgFe-LDHs were synthesized by using the co-precipitation method under standard conditions. The starting solution (with Mg/Fe molar ratio of 3.0) was prepared by dissolving $Fe(OH)_3$ (0.1333 mmol, 0.012 g) into 100 mL of 1 M HCl struvite soln. NaOH was added dropwise to the solution, while being stirred, until the pH of the solution became 9.5. The product was filtered by the Buchner filtration. The product was dried in a standard lab oven for 12 hours to prepare for XRD and Energy Dispersive X-ray (EDX) analysis.

4. Analysis & Discussion

4.1 EXPERIMENT 1.1 & 1.2 Dissolution of struvite in carbonic acid

Upon the addition of all the carbonic acid to the synthetic struvite, the pH changed from 5 to 5.5 and then to 6 in 30s seconds staying at pH 6 for 5 minutes. The pH after 24hrs had changed to pH 8 and the solution was slightly cloudy. This may have been due to the broken-down particles of struvite being suspended in the liquid and not the formation of a new product.

During the dissolution reaction of the WWTP struvite sample the pH changed from 5 to a pH of 7.5-8. No observable differences to the naked eye were noticed between the colour and nature of the powder particles after the 24hr dissolution reaction. Nucleation sites were observed at the bottom of both reaction flasks, however there was less effervescence of the carbonic acid than expected which could be the carbonic acid interreacting with the surface of the struvite particles.

SEM IMAGE ANALYSIS:

To more fully understand the struvite after the dissolution reaction, SEM images were taken of synthetic struvite crystals on the micrometre scale. The imaged struvite had euhedral, pyramidal crystals with well-formed faces and are analogous with the literature descriptions of struvite.[37] Figure 11 displays the crystal surface of struvite, which is textured but mainly uniform.

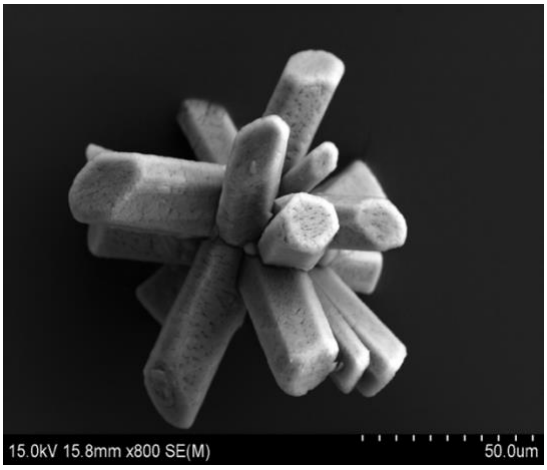

Figure 9. SEM image of a synthetic struvite crystal

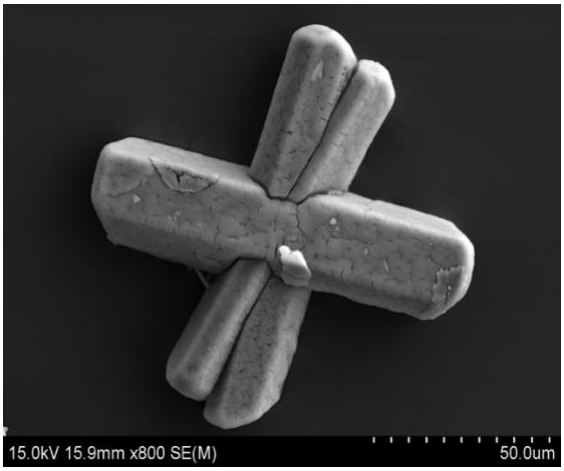

Figure 10. Synthetic struvite crystal

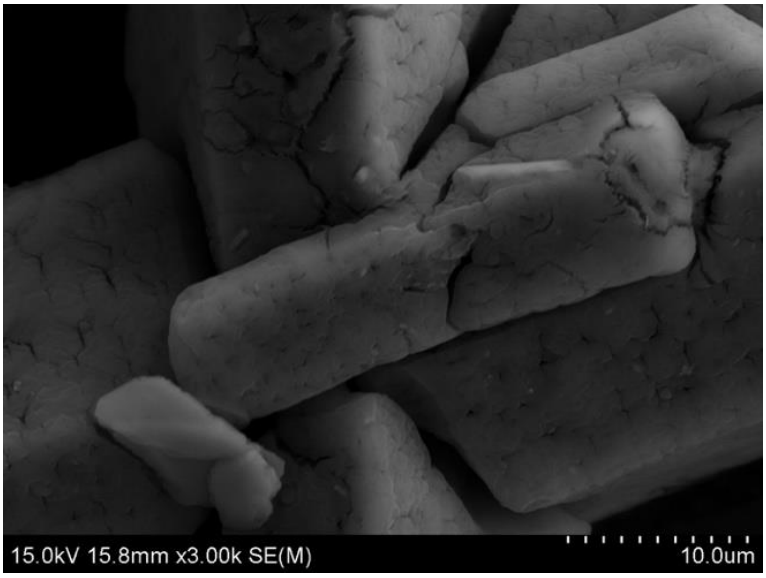

Figure 11. Crystal surface of synthetic struvite

Figure 12 and 13 depict the carbonated synthetic struvite. While there was small differences observed by the naked eye, it is clear that changes have occurred to the sample on the micro scale. A significant amount of struvite has broken off the main crystals resulting in crystal debris surrounding each main crystal. The surface of each main crystal has decreased in pyramidal nature, now displaying a more rounded appearance while the debris looks like smaller, more rectangular euhedral crystals.

Figure 12. SEM image of carbonated synthetic struvite

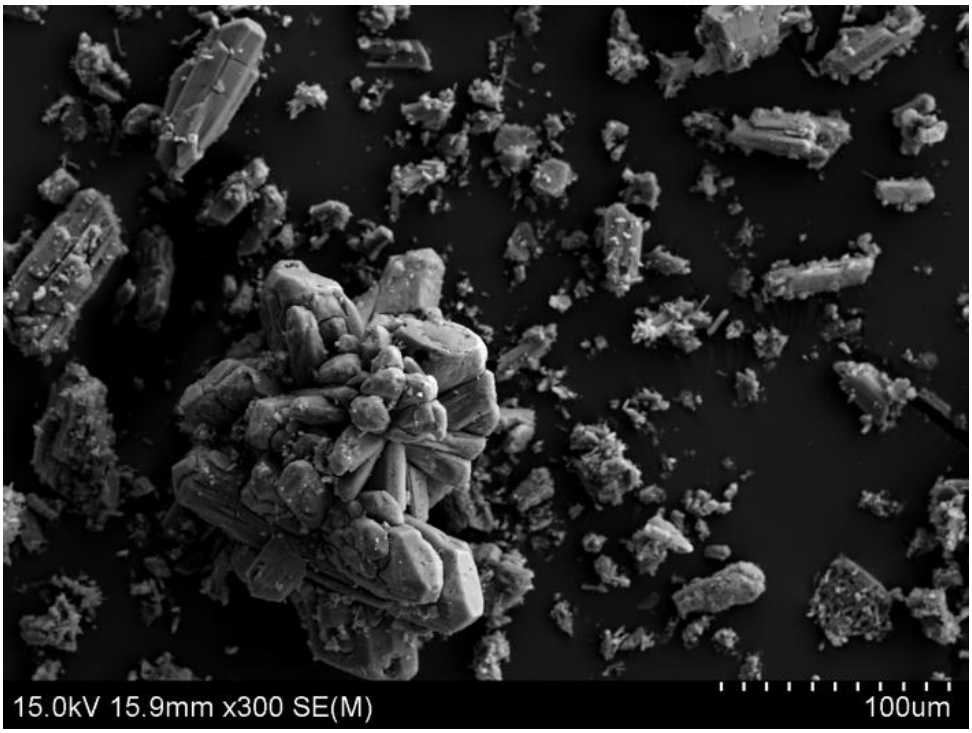

Figure 13. Crystal debris surrounding carbonated struvite crystal

Looking more closely at the crystal surface of the carbonated struvite shows that the surface has been disrupted and is not as smooth as the undissolved synthetic struvite sample.

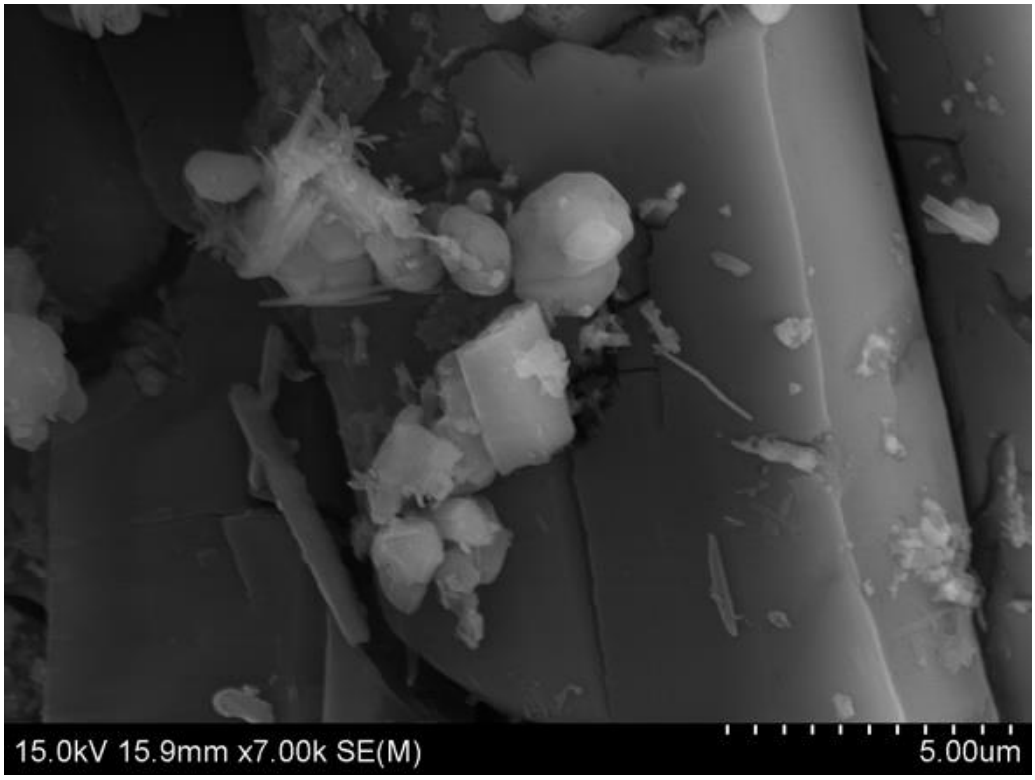

Figure 14.Crystal surface of carbonated struvite

The next four SEM images depict the WWTP struvite samples. The euhedral crystals seen in the analysis of the synthetic struvite were not observed, but this is potentially due to impurities present. The WWTP struvite samples were taken from the inside of a discharge pipe so the likelihood of impurities reacting with the struvite is very high. Significant debris surrounding the bigger chunks of the samples were also observed which is shown in Figure 17 and 18.

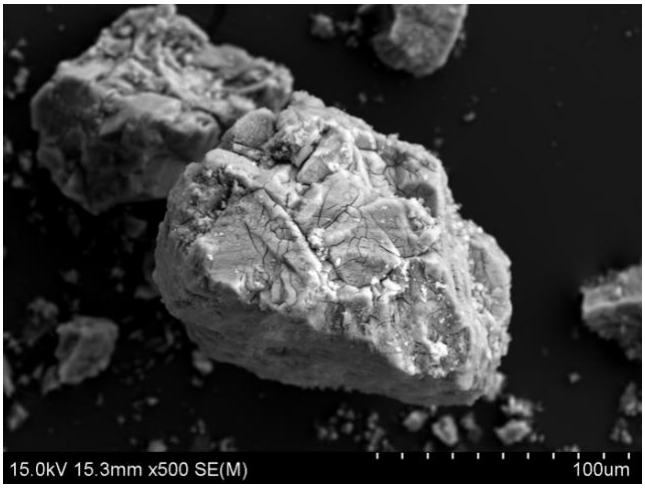

Figure 15. SEM image of a main chunk of WWTP struvite

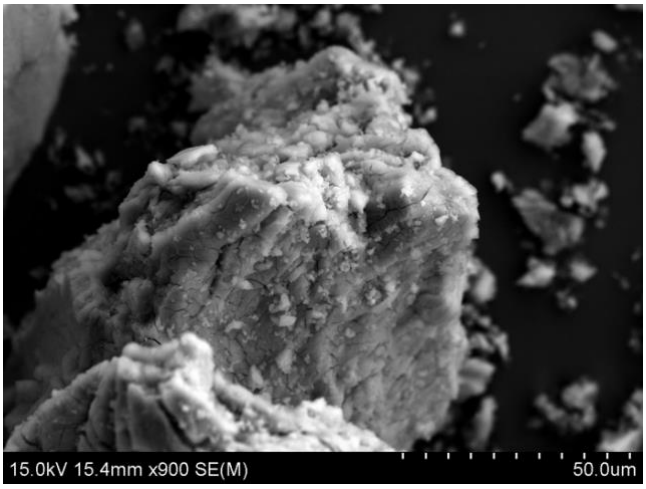

Figure 16. Close up image of crystal surface of WWTP struvite

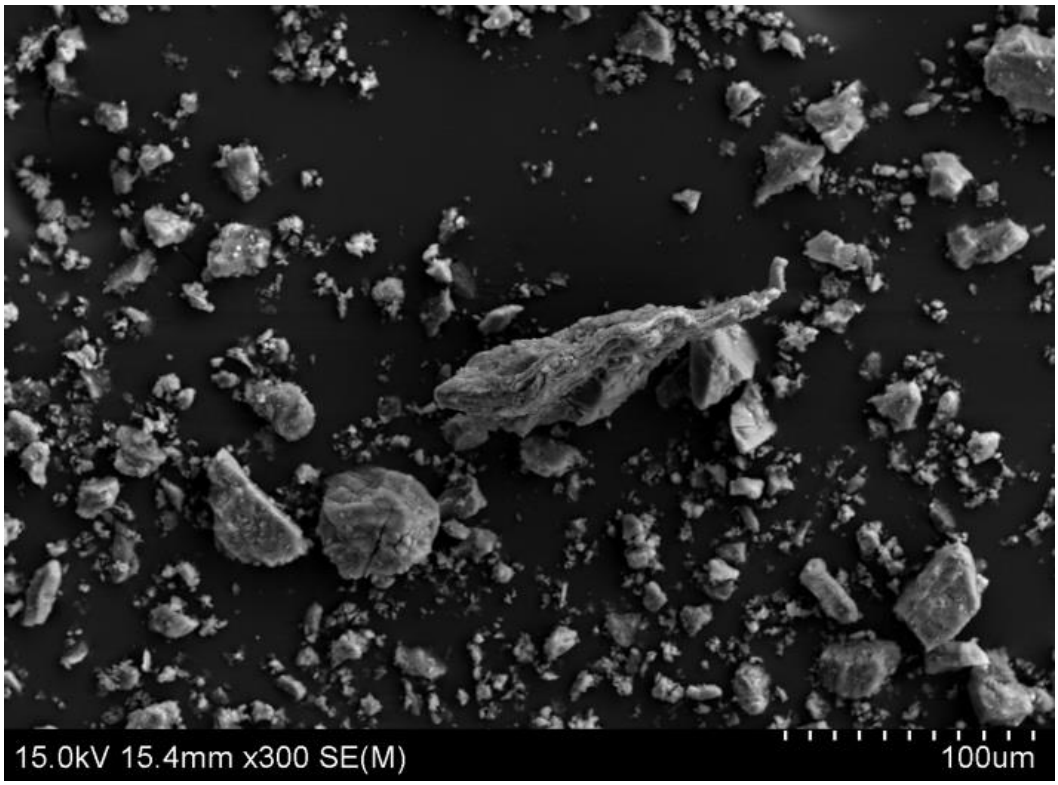

Figure 17. Smaller crystal structures in WWTP struvite samples

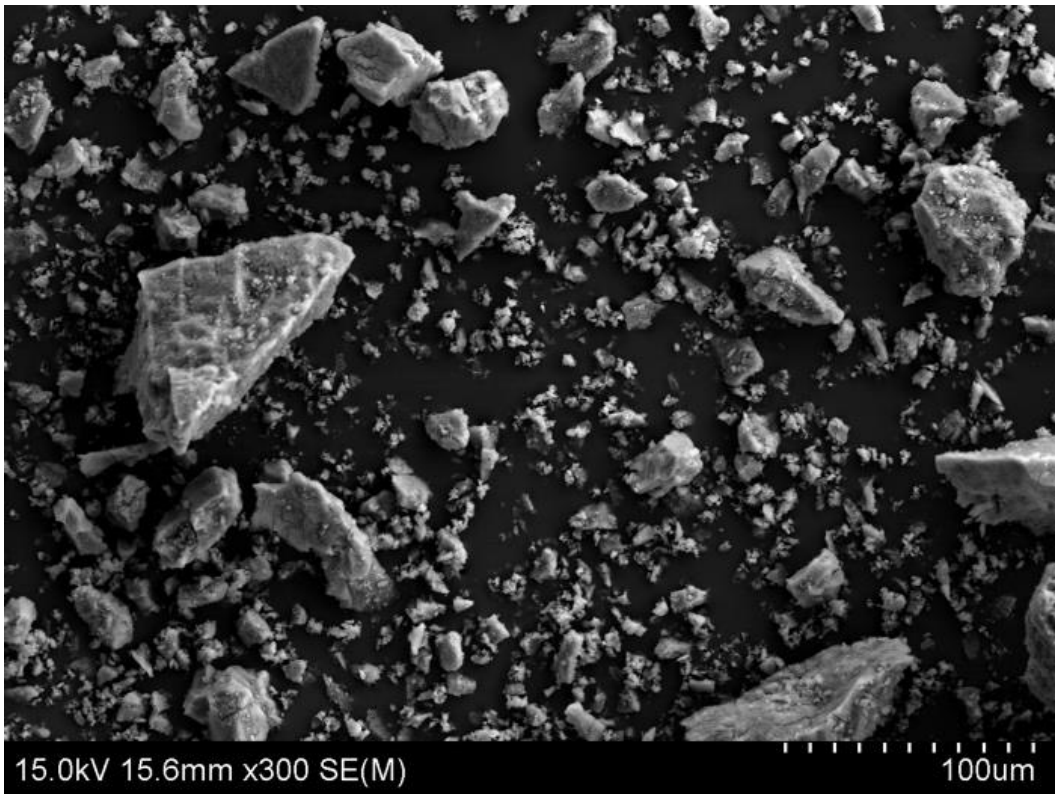

Figure 18. Crystal debris in WWTP struvite sample

Figures 19 to 21 are SEM images of the carbonated WWTP struvite. Significant changes have occurred to the sample, possibly even greater changes than the synthetic struvite which is seen in the shape of the pieces of debris around the main chunks of struvite. The debris is smaller and has a thinner rectangular, crystalline shape, which is more analogous to the real crystal shape of struvite, in comparison to the bigger, blocky shape of the debris seen in the carbonated struvite sample. This could also show that carbonic acid interacted more with the actual struvite molecules than the impurities present in the WWTP sample.

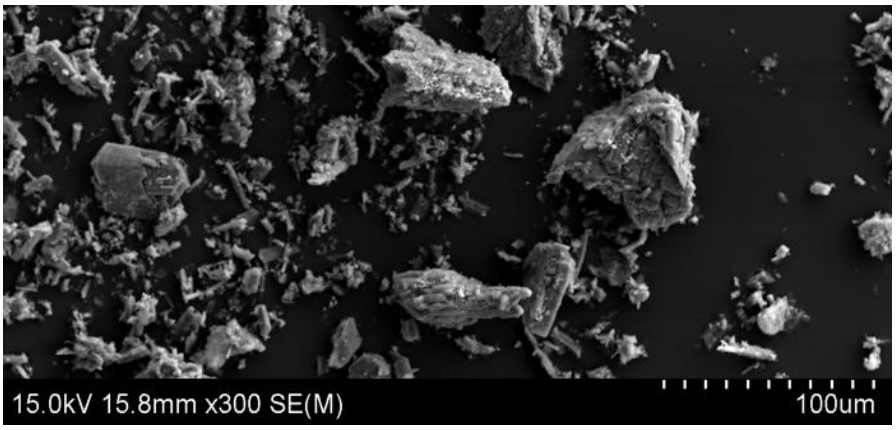

Figure 19. Crystalline debris from carbonating WWTP struvite

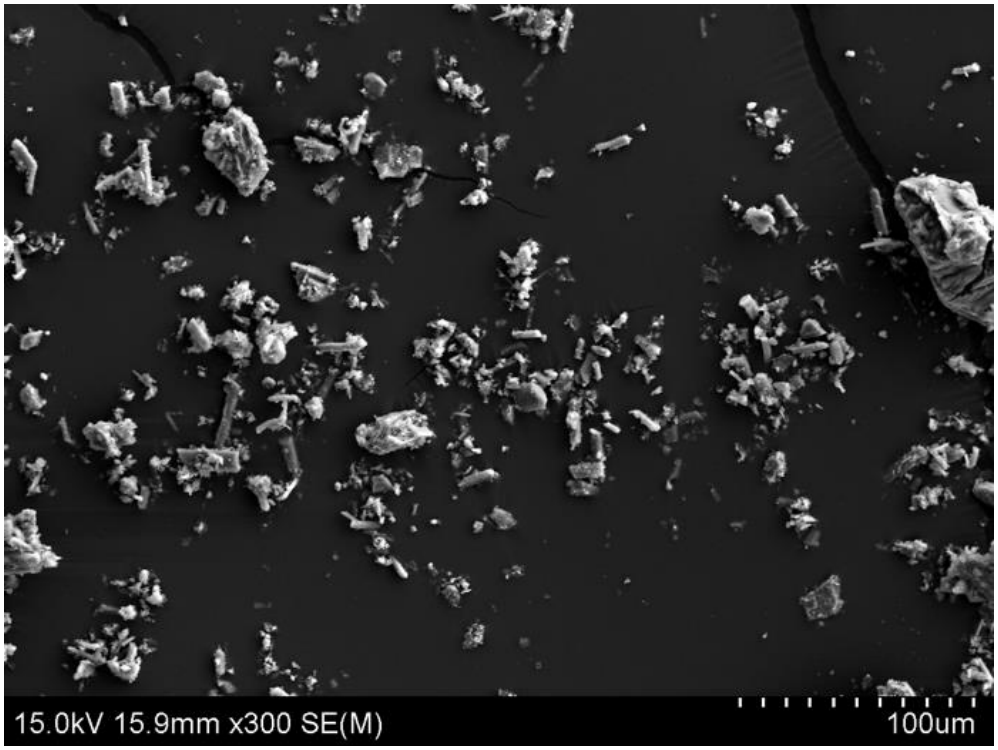

Figure 20. Rectangular crystalline debris from dissolution of WWTP struvite

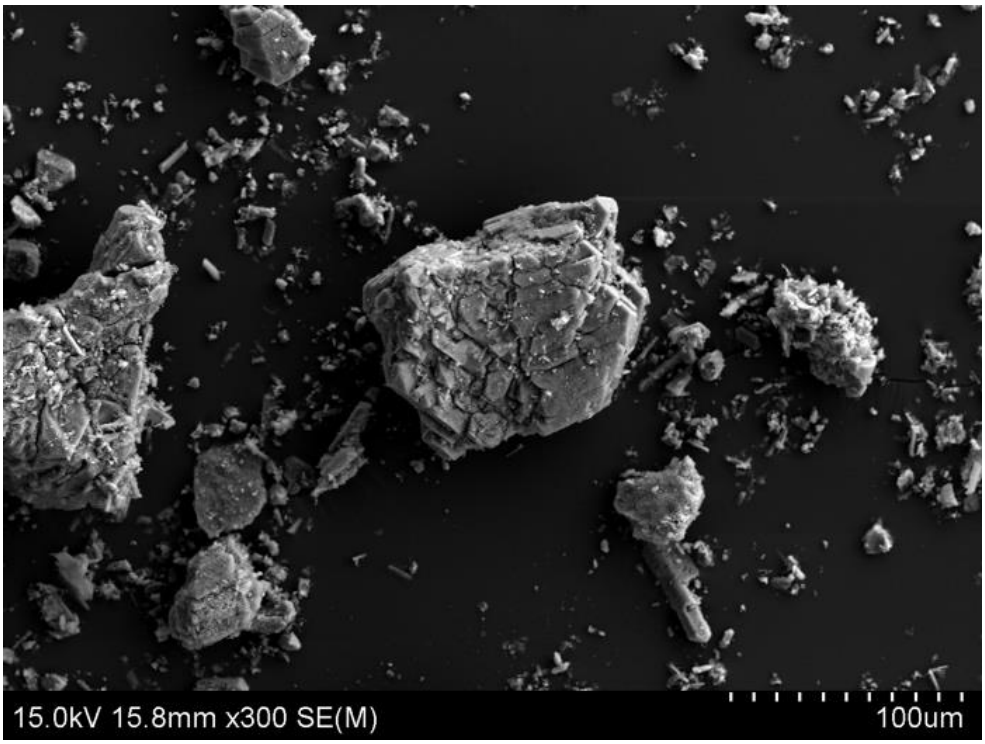

Figure 21. Carbonated WWTP struvite chunks

The crystal surface of the main chunks seen in each image is a lot more textured and rough than the smooth uniform texture seen on the synthetic struvite crystals. The shape of the main chunk in Figure 22 is particularly interesting as the long rectangular shape was not seen in any other samples imaged.

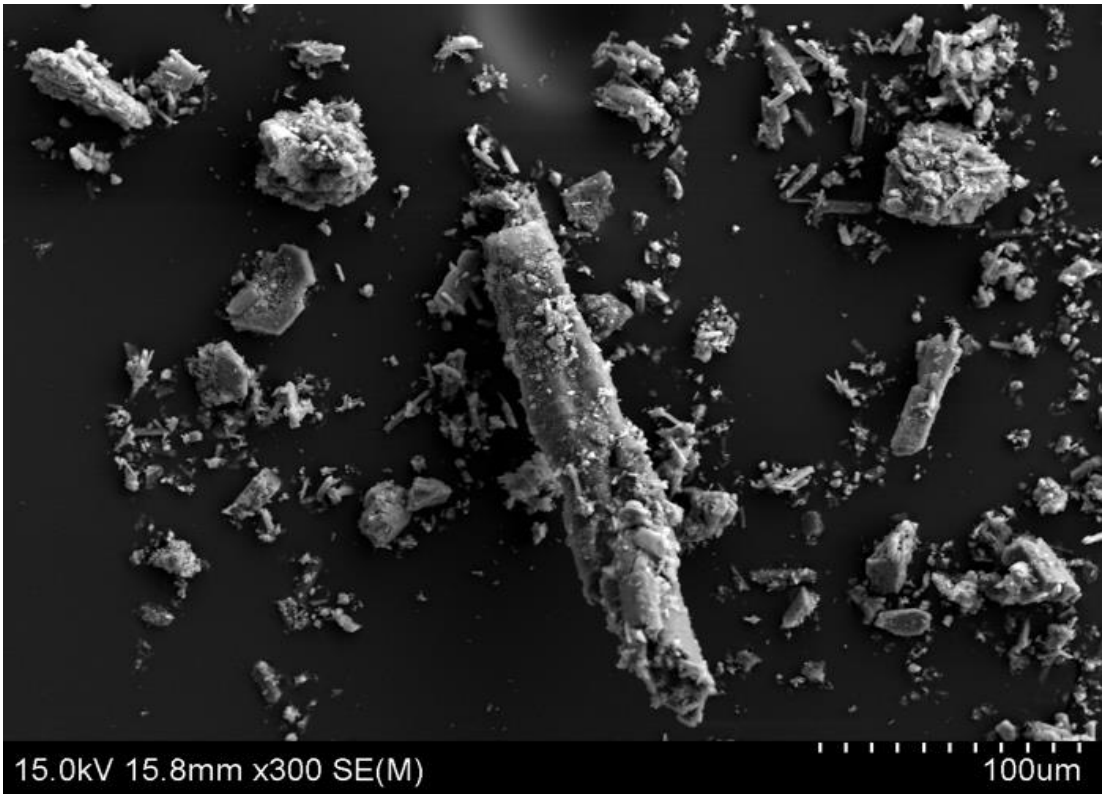

Figure 22. Carbonated WWTP struvite sample showing the differing sizes of the struvite after the reaction

XRD ANALYSIS:

Samples of the synthetic struvite, WWTP struvite and carbonated samples were analysed using XRD to check for the potential of the formation of new products. The XRD of the synthetic and WWTP samples before and after carbonation via dissolution were compared (see Figure 23 and 24). As the XRD for both samples before and after carbonation displayed the same peaks but at different intensities, this shows that no new products were formed in the dissolution reaction.

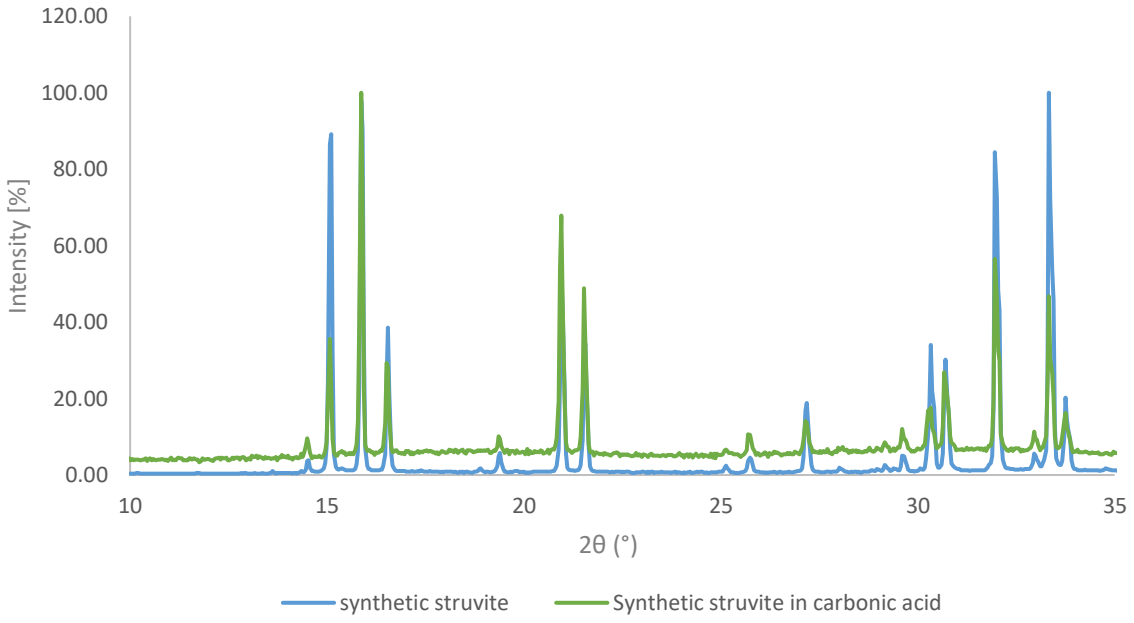

Figure 23.Dissolution of synthetic struvite with carbonic acid versus synthetic struvite

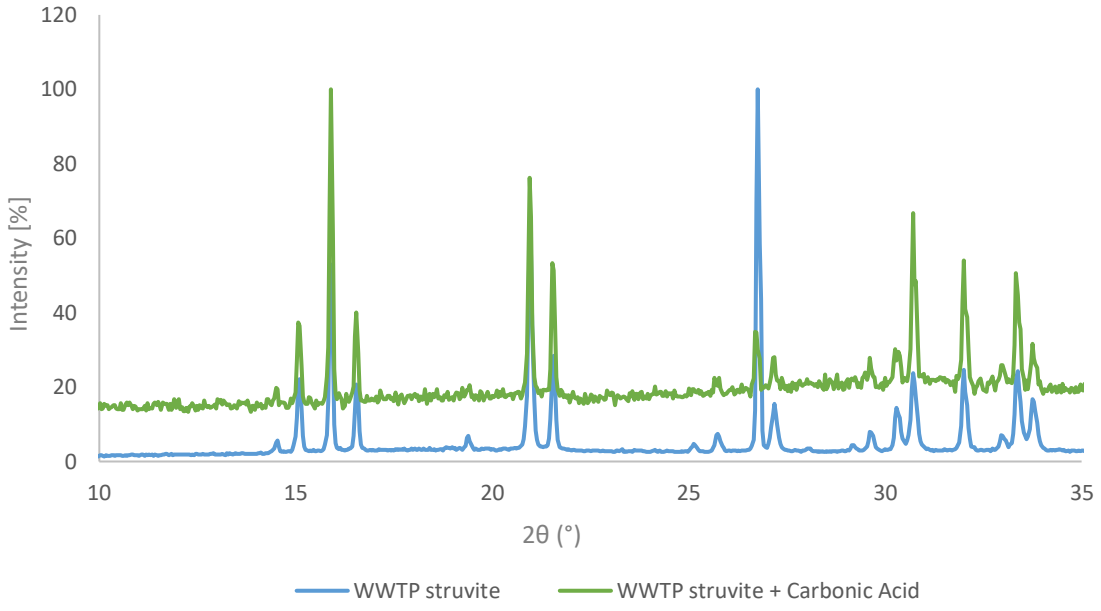

Figure 24. Dissolution of WWTP struvite with carbonic acid versus WWTP struvite

The XRD data combined with the SEM images elude to the dissolution of struvite in carbonic acid and its reprecipitation as smaller struvite crystals. The size and differing shapes of the reprecipitated crystals may be due to differing growth phases of the crystal. This is very clearly seen on the surfaces of the chunks of struvite in Figure 25. This shows that carbonic acid has the potential to dissolve struvite.

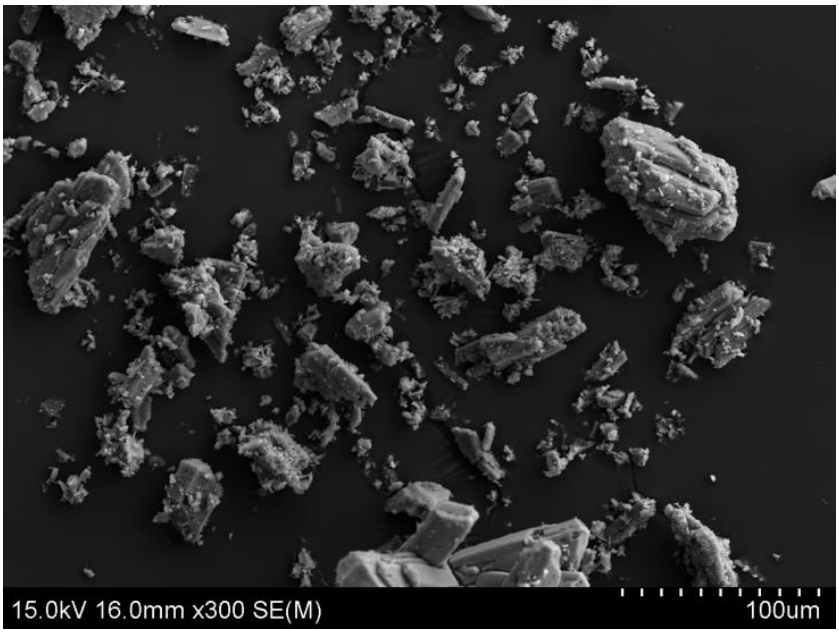

Figure 25. SEM image of carbonated synthetic struvite.

4.2 EXPERIMENT 1.3 Dissolution of chunks of struvite in carbonic acid

Chunks of WWTP struvite were also dissolved in carbonic acid of pH 5 at room temperature to see the changes to struvite chunks over time. After 72hrs the pieces of struvite had become lighter in colour and a significant amount of particles were suspended in the carbonic acid. However the chunks didn't change in size on a level observable to the naked eye.

Figure 26. Nucleation Sites on the chunks of WWTP struvite when submerged in carbonic acid

4.3 EXPERIMENT 2 Formation of ammonium bentonite

A light brown/tan powder was formed and the filtrate was colourless. The tan powder was analysed using XRD and EDX. Due to the interlayer spacing of the bentonite layers decreasing in comparison to the product, the new peak at 11.7° 2θand the lack of a peak with intensity 22.04° 2θ seen in the XRD, this product can been confirmed as ammonium bentonite, which is also seen in the XRD graphs from the reaction of 1.5x and 2x the stoichiometric ratio of sodium bentonite to the 1 M HCl struvite solution.

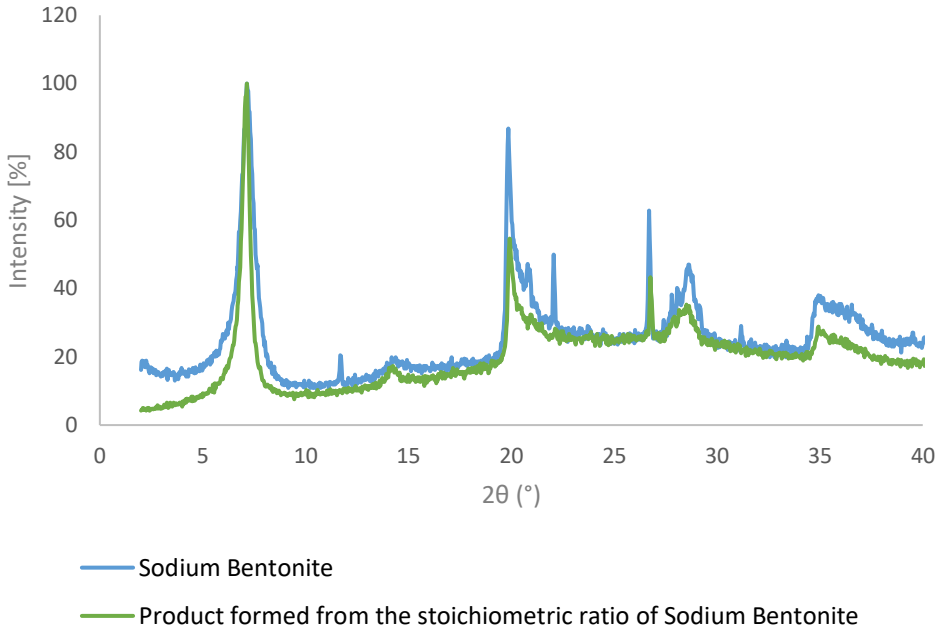

Figure 27. Comparison of the XRD of Sodium bentonite and product from 1x molar ratio in EXP 2

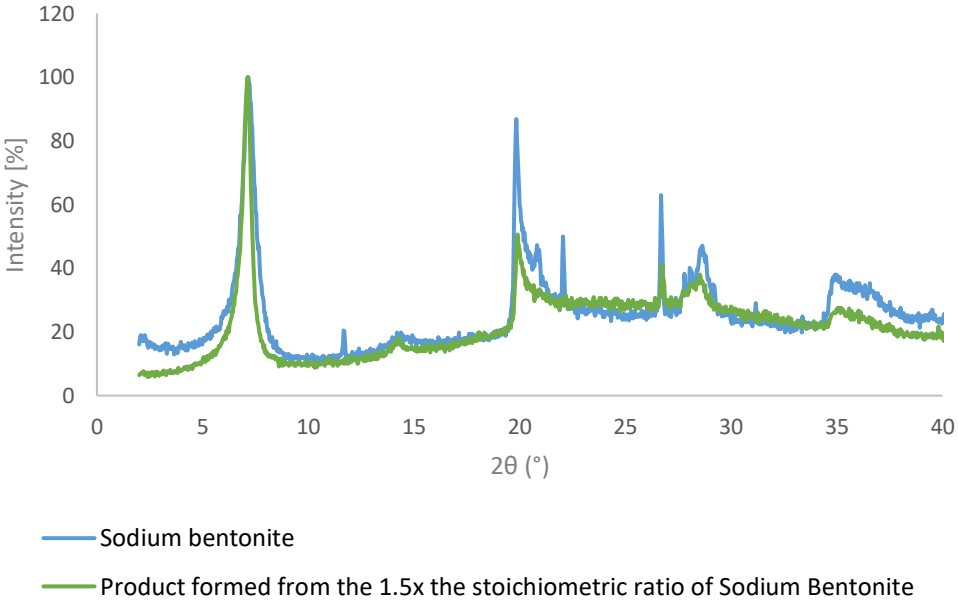

Figure 28. Comparison of the XRD of Sodium bentonite and product from 1.5x molar ratio in EXP 2

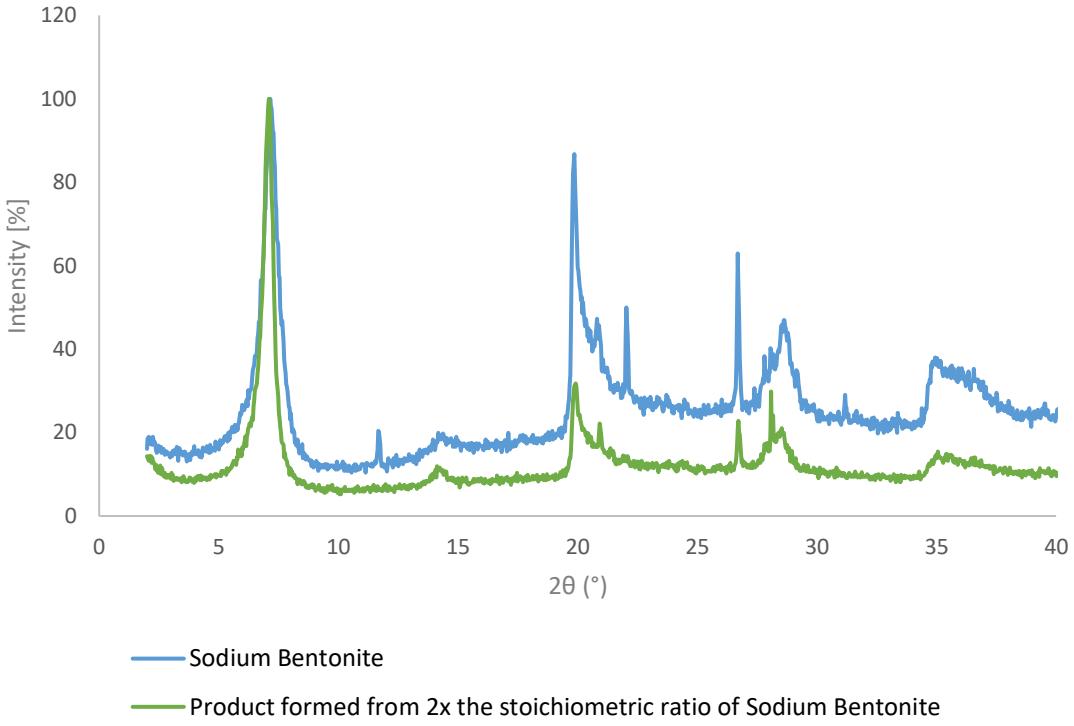

Figure 29. Comparison of the XRD of Sodium bentonite and product from 2x molar ratio in EXP 2

This is also verified by the Energy Dispersive X-ray (EDX) analysis completed on the reactant and product ammonium bentonite samples. A significant amount of nitrogen was measured relative to the very small amount of sodium, shown in Figures 30 to 32.

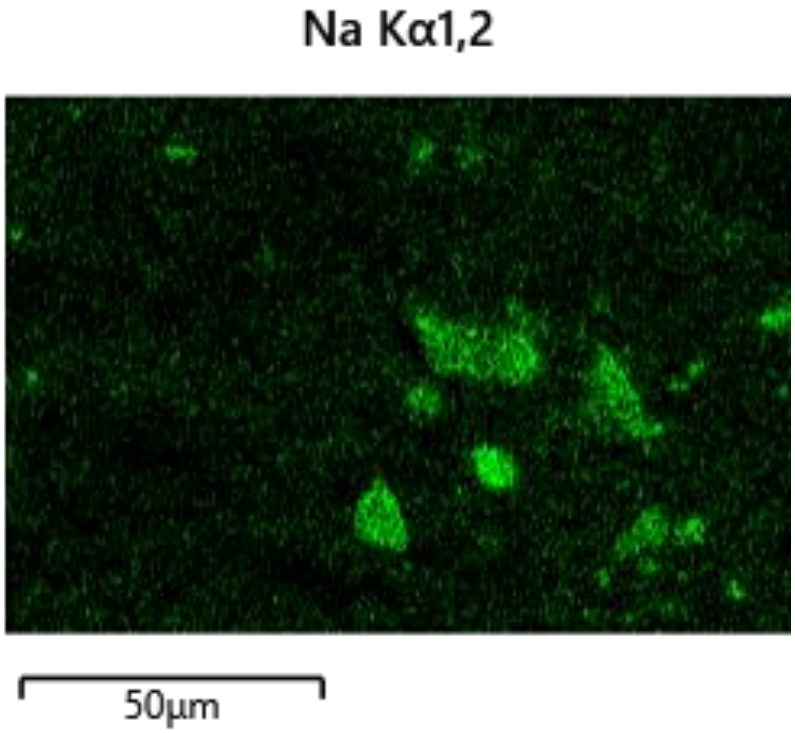

Figure 30. The amount of Na present per 50 µm in the pure sodium bentonite sample (before reaction)

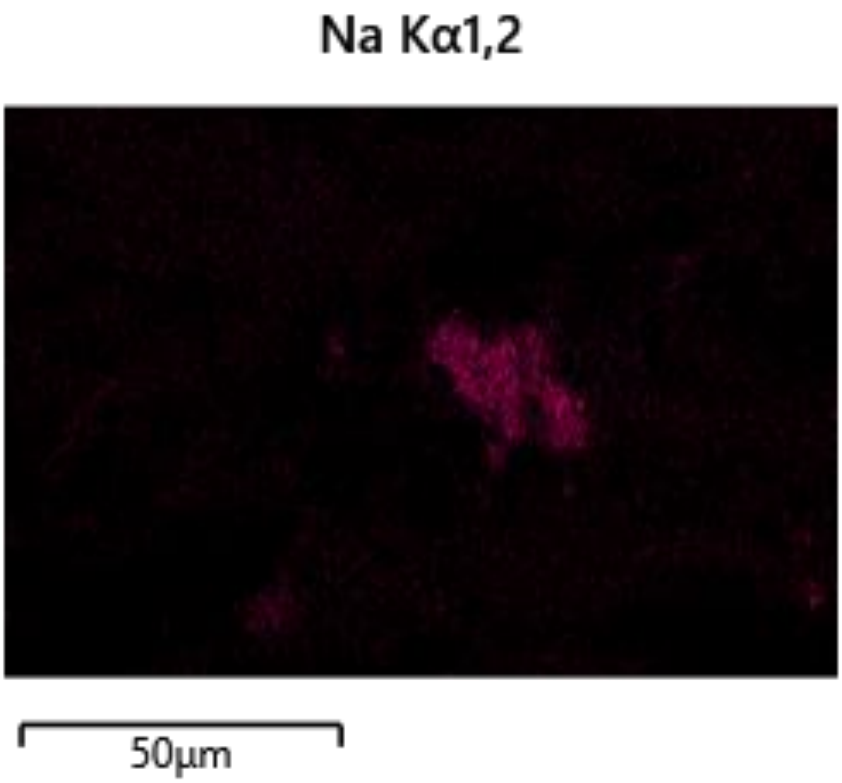

Figure 31. The amount of Na present per 50 µm in the reacted sodium bentonite sample

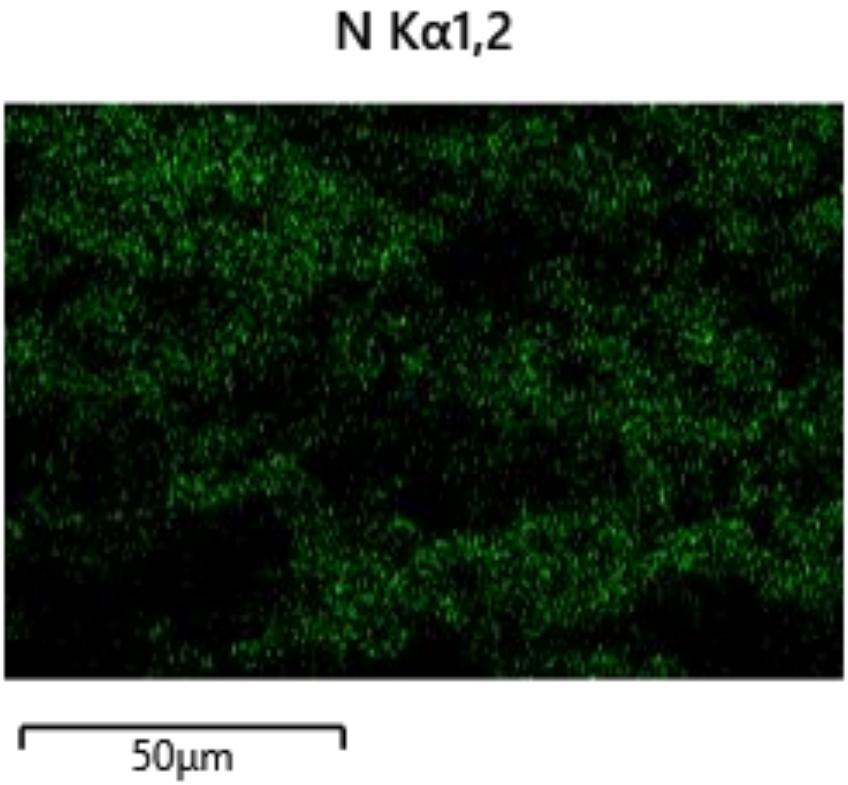

Figure 32. The amount of N present per 50 µm in the reacted sodium bentonite sample

It is similarly apparent in the comparison of the Map Sum Spectrum of the sodium bentonite sample(Figure 33) and the bentonite product (ammonium bentonite, Figure 35). Only sodium is present in Figure 33 and there is more nitrogen present than sodium in the product spectrum, which alludes to the sample being ammonium bentonite.

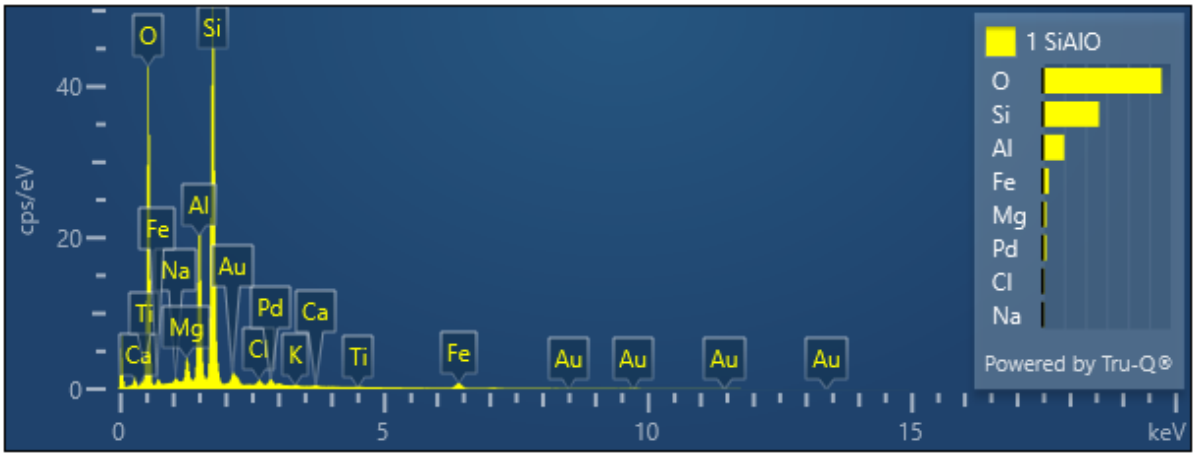

Figure 33. The EDX spectrum of elements measured in the sodium bentonite sample

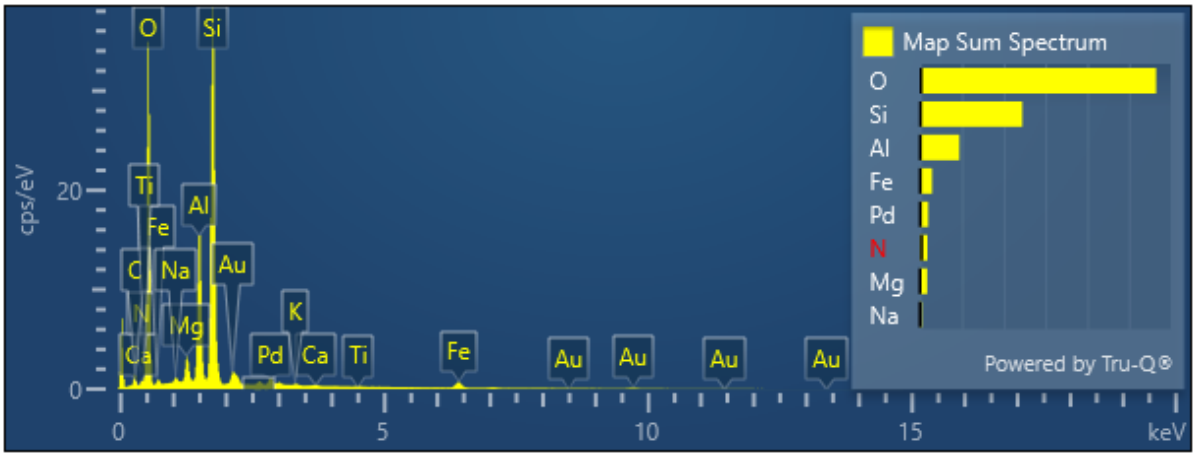

Figure 34. The EDX spectrum of elements measured in the ammonium bentonite sample

Ammonium bentonite was formed from reacting bentonite clay with the struvite 1 M HCl solution. Numerous pathways and methods could be used from this point to utilise the remaining ions in solution into useful products/chemicals.

4.4 EXPERIMENT 3 Formation of magnesium iron layered double hydroxide

The co-precipitation reaction formed a deep orange, fine powder. The powder was analysed using SEM, EDX and XRD. Figure 35 is an EDX image of the powder. It does not share similarities with the literature EDX image for MgFe-LDH (see Figure 36) which alludes to the reaction not successfully forming a MgFe-LDH. As the pH probe used in this experiment calibrated only after some difficulty, it is probable that either an excess or inadequate amount of NaOH was added during the reaction. The experiment methodology and materials needs to be adjusted to successfully complete this experiment in future attempts.

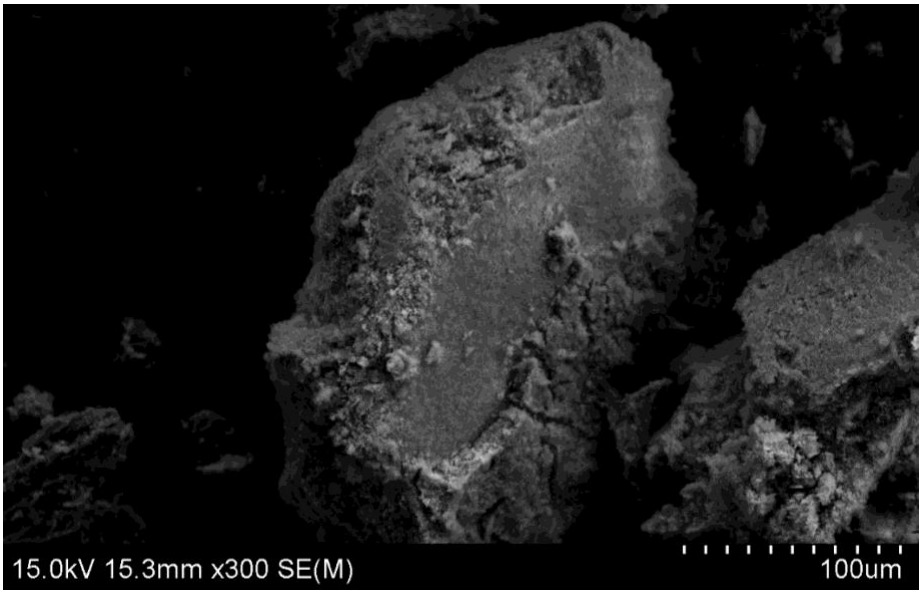

Figure 35. SEM image of product from co-precipitation reaction

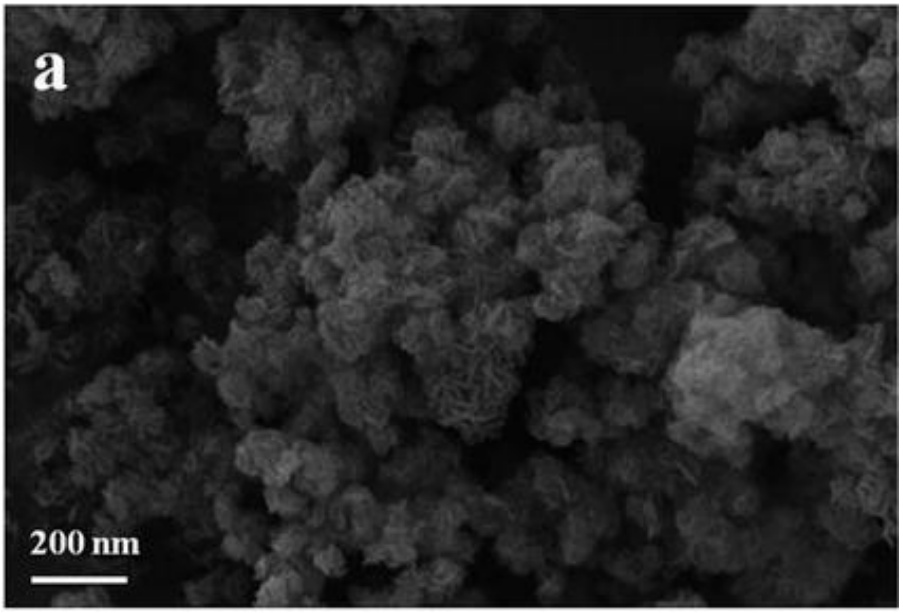

Figure 36. Literature SEM image of MgFe-LDH[38]

From the EDX images and spectrum analysis the most prevalent elements in the solution were, oxygen, silicon, iron, calcium, aluminium and phosphorous as seen in figure 37 and the map sum spectrum, figure 38.

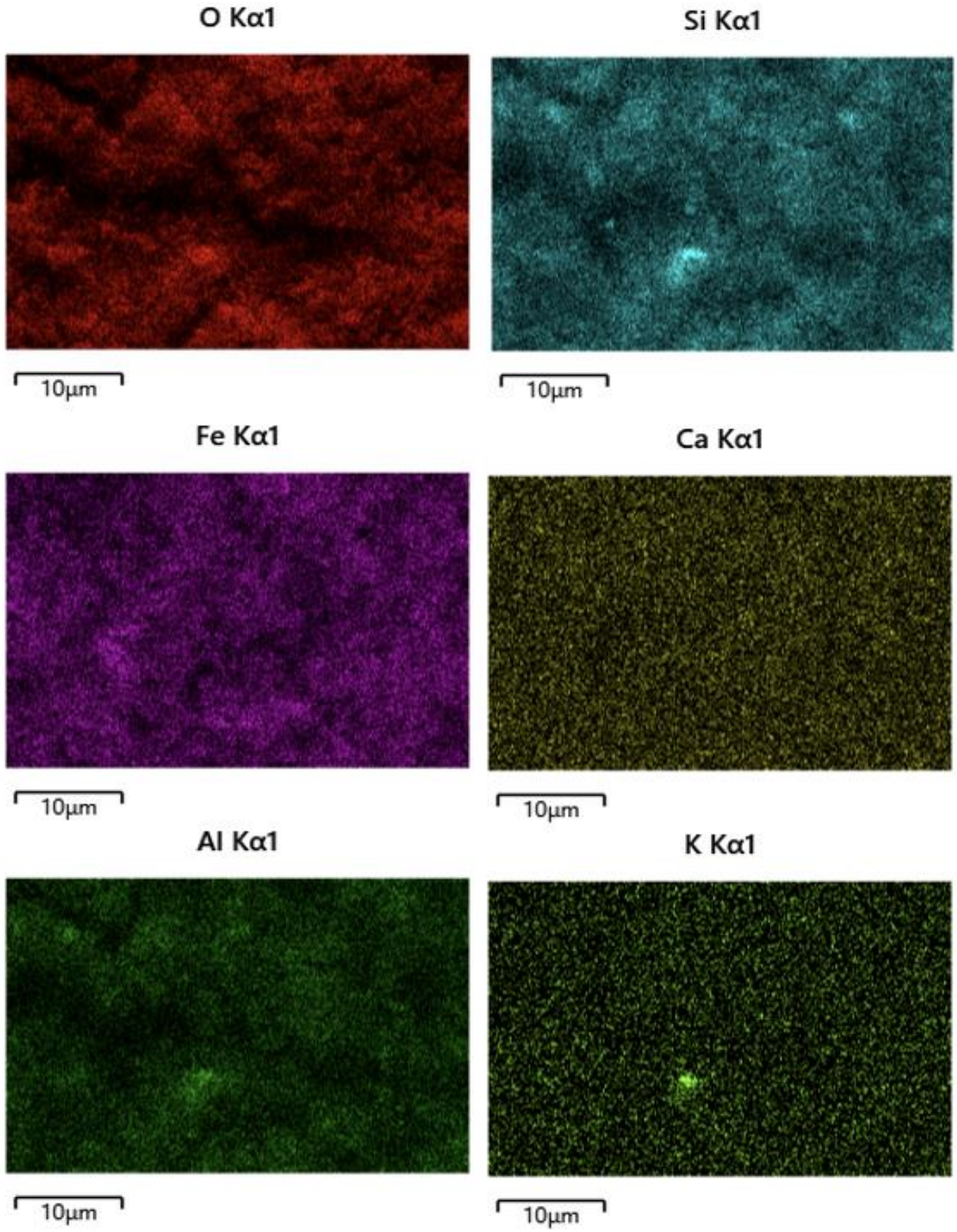

Figure 37. EDX images of co-precipitation reaction product

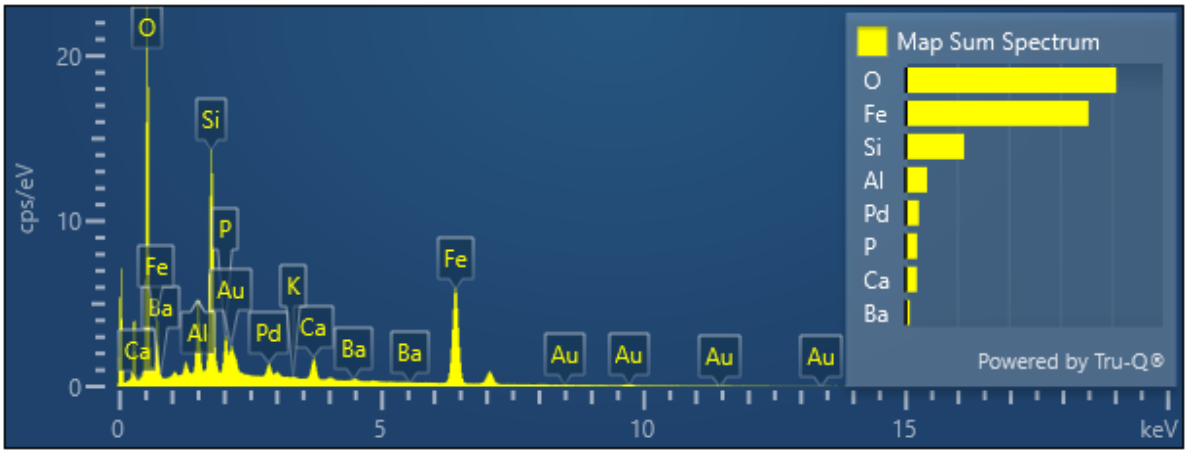

Figure 38. The EDX spectrum of elements measured in the co-precipitation LDH reaction

The XRD analysis of the co-precipitation product is analogous to the XRD analysis of sodium chloride, (see literature XRD spectrum of sodium chloride, Figure 40). As both spectra have the same core peaks at similar intensities, The product analysed was sodium chloride. This means that as well as the co-precipitation product sodium chloride also crystallised and was picked up by the XRD rather than the desired product. Therefore the washing and drying method also needs to be adjusted so only the required product is recovered.

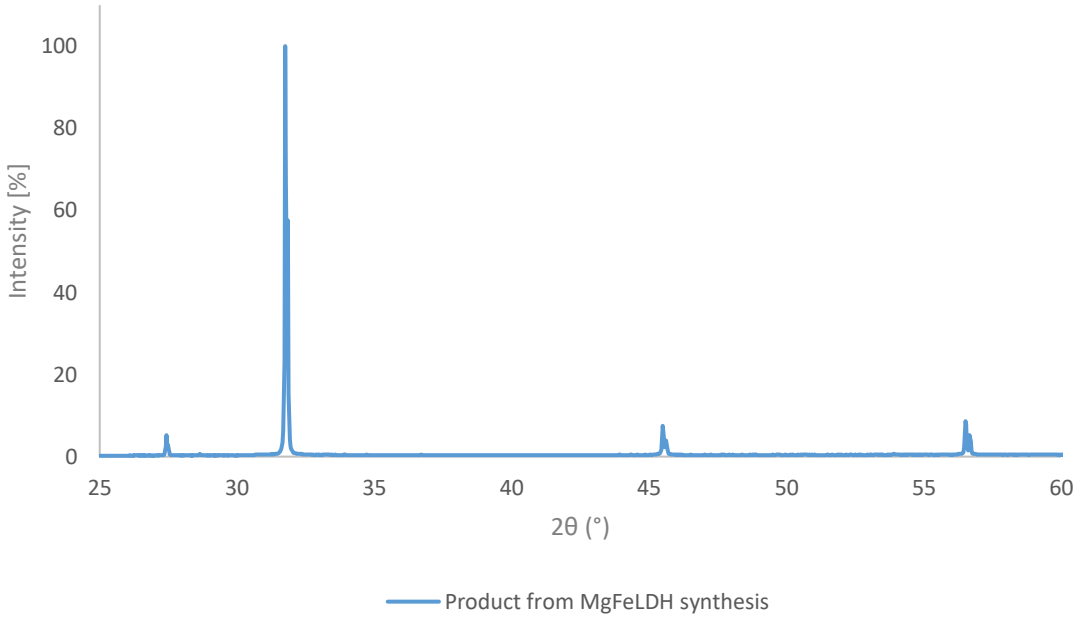

Figure 39. XRD spectrum of co-precipitation product

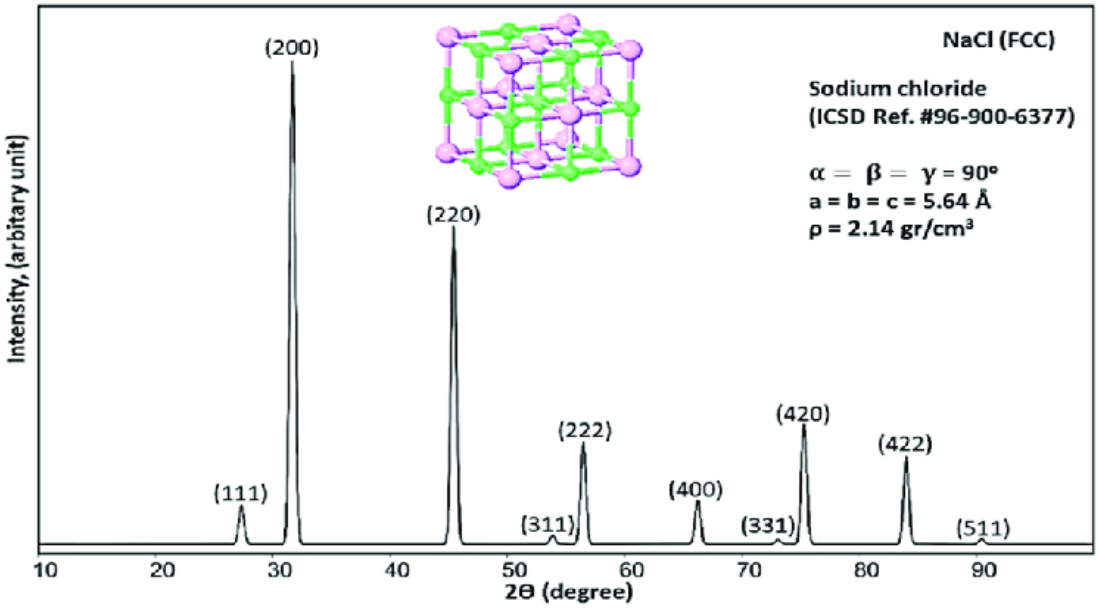

Figure 40. Literature XRD spectrum of sodium chloride[39]

5. Conclusion

The scope of this research project to investigate methods to recover ammonium, phosphate and magnesium ions from struvite was successfully completed. The dissolution of struvite in carbonic acid, (carbon dioxide is its main component and is produced onsite in WWTPs) is a method that can be used to recover ammonium, phosphate and magnesium ions in a sustainable and ethical way. This method, in conjunction with the existing research covered in Section 1.4 and the wider research, has the potential to prioritise struvite as a source of ammonium, phosphate and magnesium ions on a global level. The ideology of breaking down struvite and utilising the ion products also has the potential to be used by all wastewater treatment plants that produce struvite.

This research project has prompted the Greenwell Group to undertake further research, dissolving struvite (roughly 0.5 g being dissolved in carbonic acid at a concentration of 5-6 g/l) in a closed system, contrasting experiment 1.1 and 1.2 in this research project which dissolved struvite samples in an open system and resulted in a loss of CO_2 to the atmosphere.

5.1 Potential directions of this research:

As this was an explorative piece of science research, there are a number of areas that could be investigated in more depth:

1. Optimisation of the methodology and materials for the dissolution reaction of struvite in carbonic acid.

2. The exploration of different methodologies using carbonic acid to dissolve struvite.

3. An investigation into the implementation of these methodologies in WWTPs in collaboration with the Chemical Engineering field.

4. Exploring the supply chain process of getting the recovered ions to other sectors and industries.

5. Collaborate with environmental solicitors to understand how products formed from WWTP struvite would be legally defined and consider how the present legislation is affecting the implementation of waste repurposing schemes around the world.

6. Exploring different uses for the recovered ions notwithstanding their significant use in the fertiliser industry.

7. Testing the potential of ammonium bentonite and MgFeLDH's as fertilisers in the form of growth trials.

8. Determining a different method for the synthesis of MgFeLDH's.

9. Exploring different applications for ammonium bentonite and MgFeLDH's

10. Determining if the waste product iron ochre can be used for the synthesis of MgFeLDH's.

In conclusion, this research project has successfully achieved its objectives by investigating the recovery of ammonium, phosphate, and magnesium ions from struvite. The dissolution of struvite in carbonic acid, by utilising carbon dioxide generated on-site in WWTPs, is a promising avenue of ion recovery. When combined with other methods explored in this field and discussed in Section 1.4 the potential to utilise struvite as a source of ammonium, phosphate, and magnesium ions on a global scale becomes evident, contributing to a more sustainable and efficient use of waste materials.

Appendix

- An overview of anaerobic wastewater treatment process.

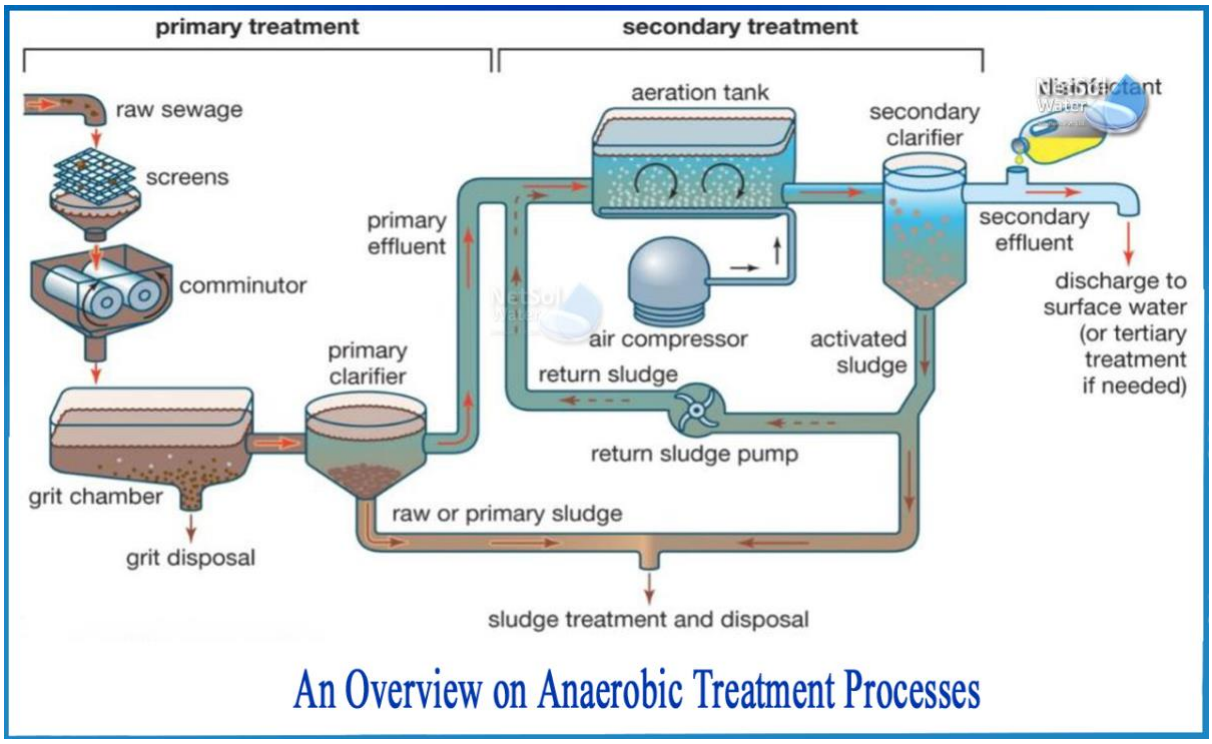

Figure 41. Wastewater treatment process flowchart[40]

- Supersaturation describes an excess amount of solute which exceeds its solubility, is the also the driving force of crystal nucleation and crystal growth.[41]

References

1. F. Abbona, M. Calleri and G. Ivaldi, *Acta Crystallogr., Sect. B: Struct. Sci.*, 1984, **40**, 223.
2. A. Whitaker and J. W. Jeffery, *Acta Crystallogr., Sect. B: Struct. Crystallogr. Cryst. Chem.*, 1970, **26**, 1429.
3. J. Prywer, L. Sieroń and A. Czylkowska, *Journal*, 2019, **9**.
4. D. Sidorczuk, M. Kozanecki, B. Civalleri, K. Pernal and J. Prywer, *The Journal of Physical Chemistry A*, 2020, **124**, 8668-8678.
5. K. P. Fattah and F. L. Chowdhury, *Journal of Environmental Engineering and Science*, 2015, **10**, 19-25.
6. B. Tansel, G. Lunn and O. Monje, *Chemosphere*, 2018, **194**, 504-514.
7. U. S. E. P. Agency, How Does Anaerobic Digestion Work?, https://www.epa.gov/agstar/how-does-anaerobic-digestion-work#:~:text=Anaerobic%20Digester%20Outputs,valuable%20outputs%3A%20biogas%20and%20digestate., (accessed August, 2023).
8. M. Logan and C. Visvanathan, *Waste Management & Research*, 2019, **37**, 27-39.
9. A. Dereszewska and S. Cytawa, *IOP Conference Series: Earth and Environmental Science*, 2021, **642**, 012012.
10. D. L. Lake, P. W. W. Kirk and J. N. Lester, *Journal of Environmental Quality*, 1984, **13**, 175-183.
11. M. F. Seleiman, A. Santanen and P. S. A. Mäkelä, *Resources, Conservation and Recycling*, 2020, **155**, 104647.
12. J. H. J. Chung-Yul Yoo, Si Young Jang, Ji Haeng Yu, Ha-Na Jeong, Chan Hee Hyeong, Hyung Chul Yoon, Jong-Nam Kim, 2013.
13. M. Capdevila-Cortada, *Nature Catalysis*, 2019, **2**, 1055-1055.
14. B. Parkinson, M. Tabatabaei, D. C. Upham, B. Ballinger, C. Greig, S. Smart and E. McFarland, *International Journal of Hydrogen Energy*, 2018, **43**, 2540-2555.
15. V. Kyriakou, I. Garagounis, A. Vourros, E. Vasileiou and M. Stoukides, *Joule*, 2020, **4**, 142-158.
16. N. Y. S. D. o. Health, The Facts About Ammonia, https://www.health.ny.gov/environmental/emergency/chemical_terrorism/ammonia_tech.htm#:~:text=How%20is%20ammonia%20used%3F,pesticides%2C%20dyes%20and%20other%20chemicals., (accessed June, 2023).

17. G. M. Peter Levi, *Journal*, 2022.
18. A. Abedin, N. Radenahmad, Q. Cheok, S. Shams, J. Kim and A. Azad, *Renewable and Sustainable Energy Reviews*, 2016, **60**, 822-835.
19. H. Malhotra, Vandana, S. Sharma and R. Pandey, 2018, DOI: 10.1007/978-981-10-9044-8_7, pp. 171-190.
20. C. f. B. Diversity, AMERICA'S FRIGHTENING PHOSPHATE PROBLEM, https://www.biologicaldiversity.org/campaigns/phosphate_mining/#:~:text=Strip%20mining%20for%20phosphate%20rock,restore%20to%20their%20natural%20state., (accessed August, 2023).
21. V. V. Ramalingam, P. Ramasamy, M. D. Kovukkal and G. Myilsamy, *Metals and Materials International*, 2020, **26**, 409-430.
22. D.-Y. Li, Y.-C. Cho, M. H. Hsu and Y.-P. Lin, *Journal of Environmental Management*, 2022, **302**, 114110.
23. M. M. T. Zin, D. Tiwari and D.-J. Kim, *Journal of Water Process Engineering*, 2021, **39**, 101697.
24. Britannica, Hydrolysis, https://www.britannica.com/science/, (accessed June, 2023).
25. M. M. Rahman, Y. Liu, J.-H. Kwag and C. Ra, *Journal of Hazardous Materials*, 2011, **186**, 2026-2030.
26. M. Lee and D.-J. Kim, *Journal of Industrial and Engineering Chemistry*, 2017, **51**, 64-70.
27. G. Morse, S. Brett, J. Guy and J. Lester, *Sci. Total Environ.*, 1998, **212**, 69.
28. G. P. Bhoi, K. S. Singh and D. A. Connor, *Water Environ Res*, 2023, **95**, e10847.
29. F. Wang, R. Fu, H. Lv, G. Zhu, B. Lu, Z. Zhou, X. Wu and H. Chen, *Scientific Reports*, 2019, **9**, 8893.
30. Y. Jaffer, T. A. Clark, P. Pearce and S. A. Parsons, *Water Research*, 2002, **36**, 1834-1842.
31. D. Kim, K. J. Min, K. Lee, M. S. Yu and K. Y. Park, *Environmental Engineering Research*, 2017, **22**, 12-18.
32. J. D. Doyle and S. A. Parsons, *Water Res.*, 2002, **36**, 3925.
33. E. Ariyanto, H. Ang and T. Sen, Proceedings from Chemeca 2011, 2023.
34. A. P. Bayuseno and W. W. Schmahl, *Environmental Technology*, 2020, **41**, 3591-3597.
35. M. Hanhoun, L. Montastruc, C. Azzaro-Pantel, B. Biscans, M. Frèche and L. Pibouleau, *Chemical Engineering Journal*, 2011, **167**, 50-58.
36. A. Miles and T. G. Ellis, *Water Sci Technol*, 2001, **43**, 259-266.

37. Struvite Mineral Data, http://www.webmineral.com/data/Struvite.shtml, (accessed June, 2023).
38. X. Wang, X. Zhu and X. Meng, *RSC Adv.*, 2017, **7**, 34984-34993.
39. M. Rabiei, A. Palevicius, A. Dashty, S. Nasiri, A. Monshi, A. Vilkauskas and G. Janušas, *Materials*, 2020, **13**, 4380.
40. N. Water, An Overview on Anaerobic Treatment Processes, https://www.netsolwater.com/an-overview-on-anaerobic-treatment-processes.php?blog=2330, (accessed September, 2023).
41. Supersaturation and Crystallization, The Driving Force For Crystallization, https://www.mt.com/gb/en/home/applications/L1_AutoChem_Applications/L2_Crystallization/Supersaturation_Application.html, (accessed September, 2023).